Hindawi Publishing Corporation
Applied Computational Intelligence and Soft Computing
Volume 2011, Article ID 692197, 9 pages
doi:10.1155/2011/692197

*Research Article*

# Null Steering in Failed Antenna Arrays

**Om Prakash Acharya, Amalendu Patnaik, and Sachendra N. Sinha**

*Department of Electronics and Computer Engineering, Indian Institute of Technology Roorkee, Roorkee 247 667, India*

Correspondence should be addressed to Amalendu Patnaik, apatnaik@ieee.org

Received 29 December 2010; Revised 21 April 2011; Accepted 16 May 2011

Academic Editor: Miin-Shen Yang



Antenna array pattern nulling is desirable in order to suppress the interfering signals. But in large antenna arrays, there is always a possibility of failure of some elements, which may degrade the radiation pattern with an increase in side lobe level (SLL) and removal of the nulls from desired position. In this paper a correction procedure is introduced based on Particle Swarm Optimization (PSO) which maintains the nulling performance of the failed antenna array. Considering the faulty elements as nonradiating elements, PSO reoptimizes the weights of the remaining radiating elements to reshape the pattern. Simulation results for a Chebyshev array with imposed single, multiple, and broad nulls with failed antenna array are presented.

## 1. Introduction

In order to reduce the effect of interfering signals, it is desirable to place nulls in specified directions during antenna beamforming. Null steering in antenna radiation pattern is very important in radar, sonar, and many other communication systems for minimizing degradation in signal-to-noise ratio (SNR) performance due to undesired interference. In active antenna arrays, a desired radiation pattern with null steering and specified SLL is achieved by determining the physical layout of the antenna array and by choosing suitable amplitude and phase of the complex excitation current for individual array elements [1]. Conventional [2–6] as well as evolutionary optimization techniques [7–15] have been used for placing nulls in antenna array patterns. In general, the null steering techniques based on controlling the excitation amplitude only, phase only, element position only, and complex weights (both amplitude and phase) have been extensively studied in the literature [2–15]. Because of the presence of large number of elements in an array, failure (not radiating) of some of the elements cannot be denied all the time. In situations, where some of the radiating elements do not radiate due to some unforeseen reasons, then the entire antenna pattern gets distorted. It degrades the SLL and destroys the pattern null created to suppress the interference from particular directions. The replacement of the defective element of the array is not possible in every situation. Instead, reconfiguration of the amplitude and phase of the remaining elements can partially compensate for the failed elements and, thus, maintain the desired SLL and nulling performance.

If all array elements are fully functional, then analytic techniques can be used to find the optimum excitations of each element to yield the desired pattern. But for a failed array, it is very difficult to find an analytical approach for the compensation problem, because with the presence of defective elements the symmetry fails. Literature survey reveals the implementation of this compensation problem with numerical techniques which produces a pattern with minimal loss of quality. Array failure correction was considered by Mailloux [16–18] in digital beamforming arrays to combat interfering sources. Peters [19] employed the conjugate gradient method to correct element failures. Zainud-Deen et al. [20] have used orthogonal method for the same problem. Levitas et al. [21] have introduced a practical, suboptimal compensation technique. Recently, Genetic Algorithm (GA) [22, 23] and Simulated Annealing (SA) [24] techniques have been used for correcting element failures in antenna arrays. Hybrid optimization method [25, 26] has been applied to improve the array pattern in the presence of failed elements. These compensation methods for the defective elements improve the pattern of array by re-optimizing the weights of the

functional elements. In all the above approaches only SLL issue was addressed, but the null steering problem in failed arrays was not addressed.

In the present paper, we have attempted to show the feasibility of using failed antenna array as a normal array and concentrated on the null steering and SLL suppression issues. Instead of an analytical approach, an evolutionary optimization technique, namely, PSO [27–30] was used to reoptimize the excitation of the working elements. The reason of choosing PSO is that, this stochastic evolutionary computation technique, based on the movement and intelligence of swarms, has been shown in certain instances to outperform other methods of optimization like GA [31]. The computational time taken by PSO to arrive at the desired solution is less compared to GA. A linear Chebyshev array was taken as the candidate antenna and tested for the developed methodology. It can be extended to planar arrays also.

## 2. Problem Formulation

The far-field pattern of an $N$-element linear array, equally spaced, nonuniform amplitude, and progressive phase excitation is given by [1]

$$F(\theta) = \frac{\mathrm{EP}(\theta)}{F_{\max}} \sum_{n=1}^{N} w_n e^{j(n-1)kd\cos\theta}, \tag{1}$$

where $w_n$ accounts for the nonuniform current excitation of each element. The spacing between the elements is $d$, $\theta$ is the angle from broad side. $\mathrm{EP}(\theta)$ is the element pattern ($\mathrm{EP}(\theta) = 1$ for isotropic source), and $F_{\max}$ is peak value of far field pattern.

Element failure in antenna arrays degrade the null regions and also cause sharp variations in the field intensity, increasing both sidelobe and ripple level of power pattern. In the present work in addition to the SLL suppression, maintenance of the null position was carried out for the defected array. So the goal was to determine the weights of the working elements of array to maintain the null performance and to restore the peak SLL of a damaged array close to the original one in the presence of element failure. We have assumed the failure as complete, that is, no radiation from the defected element. The PSO was applied to recover the SLL and to maintain the null position according to the required specifications. It minimizes the following cost function, $I$, and returns optimum current excitations for the unfailed elements that will lead to the desired radiation pattern with reduced SLL and the null at desired position

$$I = \sum_{\theta=-90^\circ}^{90^\circ} [W(\theta)|F_{\mathrm{PSO}}(\theta) - F_d(\theta)|] + \frac{1}{N_{\mathrm{tot}}} \sum_{i=1}^{N_I} [|F_{\mathrm{PSO}}(\theta_i)| - \mathrm{Mask}(\theta_i)]^2. \tag{2}$$

The first term in the cost function is meant for interference suppression, that is, to place nulls at specified directions, in the presence of faulty elements, where, $F_{\mathrm{PSO}}(\theta)$ is the pattern obtained by using PSO, $F_d(\theta)$ is the desired pattern, and $W(\theta)$ is the controlling parameter for creating the null.

The second term of the cost function in (2) is used for the purpose of SLL reduction, where Mask is an upper bound on the array factor enforcing a peak sidelobe power of $-30$ dB in the region $|\theta| \geq 8^\circ$. The main lobe region is defined as the region $|\theta| \leq 8^\circ$. In this region the Mask is valued as 0 dB. $F_{\mathrm{PSO}}(\theta)$ is computed using the samples $\theta_i$ of size $N_I$ which exceeds the level of Mask and is normalized by the total number of samples $N_{\mathrm{tot}}$ used to sample the entire range. Figure 1 shows both the original Chebyshev array pattern and the mask used in the cost function to restore the pattern.

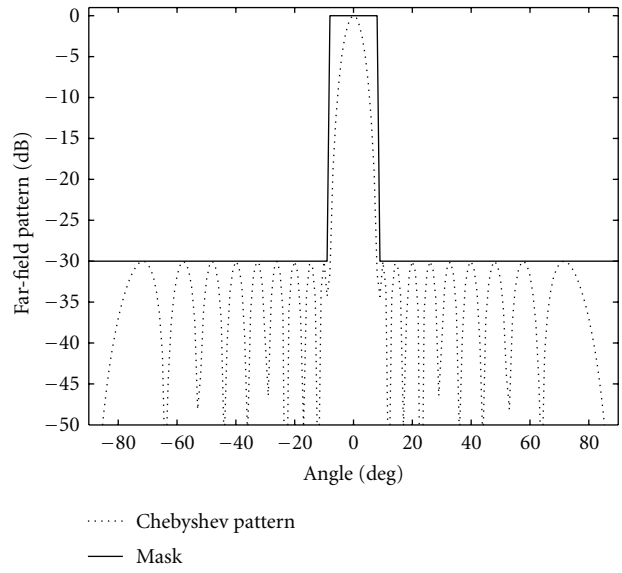


Figure 1: Chebyshev array pattern and the mask used for corresponding damaged pattern.

## 3. Particle Swarm Optimization

PSO is an evolutionary computational technique based on the movement and intelligence of swarms introduced by Kennedy and Eberhart in 1995 [27]. It is simple to apply, easy to code, and is capable of solving difficult multidimensional optimization problems efficiently. It has already been applied successfully for solving many electromagnetic problems [30]. Although the PSO technique has been described in the literature in length, but for completeness of the paper, here we have briefly described the technique.

According to PSO terminology, every individual swarm is called a particle. Initially the particles are placed within a space with the dimensions equal to the number of design parameters used in the optimization. The performance of each particle is measured according to the mathematical function called "cost function" within the solution space. A cost function is a measure of the deviation from the desired value. All the particles move in a search space and update their velocity according to the best position already found by

themselves, that is, personal-best and by their neighbors, that is, global-best, and try to find an even better position.

In the present application of PSO, 30 initial particles were taken and they were manipulated according to the following equation:

$$v_{n+1} = wv_n + c_1\text{rand}(\,)(p_{\text{best},n} - x_n) + c_2\text{rand}(\,)(g_{\text{best},n} - x_n), \tag{3}$$

where $v_n$ is the velocity of the particle in the $n$th dimension and $x_n$ is the particle's coordinate in the $n$th dimension. The parameter $w$ is the inertial weight, that specifies the weight by which the particle's current velocity depend on its previous velocity. $p_{\text{best}}$ and $g_{\text{best}}$ are the personal-best and global-best positions, respectively, $c_1$ and $c_2$ are two scaling factors which determine the relative pull of $p_{\text{best}}$ and $g_{\text{best}}$, and rand( ) is a random function in the range [0, 1].

Once the velocity has been determined, it is easy to move the particle to its next location. The velocity is applied for a given time-step $\Delta t$ and the new coordinate $x_n$ is computed as

$$x_{n+1} = x_n + \Delta t \times v. \tag{4}$$

During this iterative process, the particles gradually settle down to an optimum solution.

## 4. PSO Implementation and Results

For the implementation of the developed methodology, a 20-element linear Chebyshev array with $\lambda/2$ interelement spacing was taken as the test antenna. Standard analytical procedure was applied to find the nonuniform excitations for a $-30$ dB sidelobe level in the Chebyshev array as shown in Figure 1. The null steering was performed for single, multiple, and sector nulls in the imposed directions by recalculating the amplitude and phase of each array element by using PSO algorithm. Then some of the array elements were considered as failed elements by equating their excitations to zero. It was observed that the nulling performance was degraded significantly. In order to obtain desired nulling pattern with failed elements which has a good parity with the pattern as before, the excitations of the remaining working elements were adjusted by PSO. The proposed method was validated by considering few examples of pattern synthesis with null steering of a linear antenna array with defective elements.

In the PSO optimization process, to obtain the nulling performance in a failed antenna array the complex weight of each working element was considered as the optimization parameter. In the present problem, a population size of 30 was chosen. The parameter $w$, the inertial weight, was linearly damped with iterations starting with a value of 0.9 and decreased linearly to 0.4 at the last iteration. $c_1$ and $c_2$, two constants called cognitive parameter and social parameter, were fixed at 2.

*Case 1* (recovery of single null with element failure). In this case, it was assumed that the single null of the fully functional array was at 20° direction. Figure 2 shows the corresponding radiation pattern created by modifying the excitations of the array elements. At the first instant the element failure in the array was considered with defective elements at 3rd and 18th position. With this the sidelobe was increased by around 10 dB and existing null was destroyed. Then the developed PSO formulation was applied for recovery of the pattern. The performance of PSO for this case is demonstrated in Figure 3 for a broadside array. As can be clearly seen from the figure, in addition to the SLL reduction, the null was recovered at its previous position, that is, at 20°. The value of different parameters in the cost function were selected as $F_d(\theta) = 0$, for $\theta = \theta_i$, $W(\theta) = 100$, for $\theta = \theta_i$ and $W(\theta) = 1$, for other directions. The convergence curve for this case, with the progress of PSO iterations is shown in Figure 4.

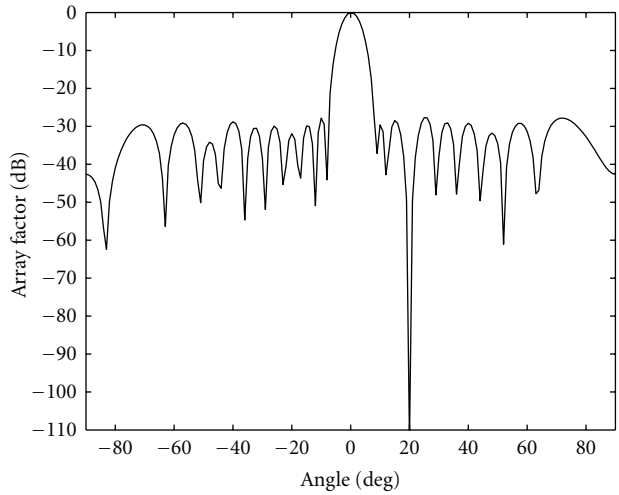


Figure 2: Radiation pattern of 20 element linear broadside array with null at 20° and SLL of −30 dB.

This method of finding the excitations can easily be extended for the patterns with main beam directed at any angle. Figure 5 shows the pattern of the 20 element linear array with a null at 20°, main beam directed at −30° and the SLL maintained at −30 db. The formulation was applied for the failed array with faults at the same positions, that is, 3rd and 18th elements. The recovered pattern after applying the PSO formulation is shown in Figure 6.

In order to study the performance of pattern recovery with more number of faulty elements, four faults were created at 2nd, 3rd, 18th, and 19th elements in the same Chebyshev array with a single null. The degraded and the recovered pattern for this scenario are shown in Figure 7. Comparison of this figure with Figure 3 reveals that the depth of the null in the recovered pattern decreases with increase in the number of faulty elements.

The element excitations for single null recovery with two and four element failures are shown in Table 1 along with the element excitations for the array with single null at 20° without faulty elements. A comparison of the null depth level (NDL) and maximum SLL in the recovered patterns discussed under Case 1 is shown in Table 2.

*Case 2* (recovery of double null with element failure). Chebyshev pattern with double nulls placed at $\theta_1 = -42°$

Table 1: Element excitations corresponding to Case 1.

| Element position | Single null at 20° without any fault | | Recovery of null with two faults at 3rd and 18th position | | Recovery of null with four faults at 2nd, 3rd, 18th and 19th position | |
|---|---|---|---|---|---|---|
| | Amplitude | Phase (Deg) | Amplitude | Phase (Deg) | Amplitude | Phase (Deg) |
| 1 | 0.2528 | 0.0887 | 0.0183 | 5.0180 | 0.0493 | 7.9004 |
| 2 | 0.2498 | 3.2166 | 0.1109 | 2.3413 | **0.0000** | **0.0000** |
| 3 | 0.3713 | 1.7141 | **0.0000** | **0.0000** | **0.0000** | **0.0000** |
| 4 | 0.5084 | 2.2080 | 0.2727 | 2.6761 | 0.3252 | 3.6915 |
| 5 | 0.6307 | 0.4111 | 0.4391 | 2.1064 | 0.4086 | 6.1520 |
| 6 | 0.7114 | 0.2294 | 0.5917 | 4.4168 | 0.6109 | 5.7187 |
| 7 | 0.7839 | 0.5271 | 0.7583 | 1.5168 | 0.7446 | 4.2470 |
| 8 | 0.8678 | 0.2244 | 0.8502 | 2.3563 | 0.8904 | 1.8244 |
| 9 | 0.9374 | 0.4477 | 0.9469 | 1.0522 | 0.9640 | 0.3368 |
| 10 | 1.0000 | 0.0560 | 1.0000 | 1.3101 | 1.0000 | 0.0005 |
| 11 | 1.0000 | 0.0560 | 1.0000 | 1.3101 | 1.0000 | 0.0005 |
| 12 | 0.9374 | 0.4477 | 0.9469 | 1.0522 | 0.9640 | 0.3368 |
| 13 | 0.8678 | 0.2244 | 0.8502 | 2.3563 | 0.8904 | 1.8244 |
| 14 | 0.7839 | 0.5271 | 0.7583 | 1.5168 | 0.7446 | 4.2470 |
| 15 | 0.7114 | 0.2294 | 0.5917 | 4.4168 | 0.6109 | 5.7187 |
| 16 | 0.6307 | 0.4111 | 0.4391 | 2.1064 | 0.4086 | 6.1520 |
| 17 | 0.5084 | 2.2080 | 0.2727 | 2.6761 | 0.3252 | 3.6915 |
| 18 | 0.3713 | 1.7141 | **0.0000** | **0.0000** | **0.0000** | **0.0000** |
| 19 | 0.2498 | 3.2166 | 0.1109 | 2.3413 | **0.0000** | **0.0000** |
| 20 | 0.2528 | 0.0887 | 0.0183 | 5.0180 | 0.0493 | 7.9004 |

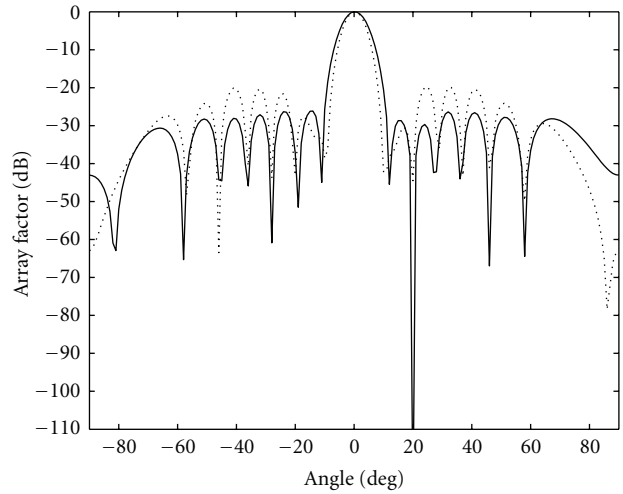


Figure 3: Radiation pattern for 3rd and 18th element failure with main beam at broadside. Dotted line curve shows the damaged array pattern and the solid line curve shows the corrected pattern.

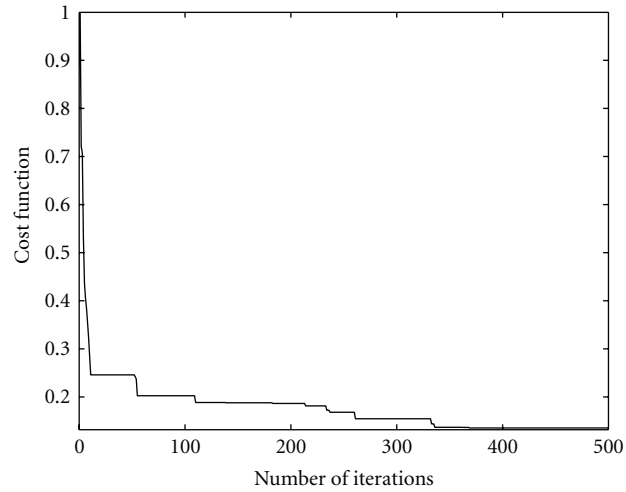


Figure 4: Convergence curve for recovery of single null in the presence of two faulty elements.

Table 2: Comparison of NDL and SLL for the configurations discussed in Case 1.

| | Without any fault | With failure of two elements | With failure of four elements |
|---|---|---|---|
| NDL (dB) | −137 | −117 | −91.01 |
| SLL (dB) | −27.94 | −25.98 | −23.41 |

and $\theta_2 = 18^\circ$ were achieved by optimizing the current excitations of the array elements (Table 3). The corresponding pattern is shown in Figure 8. The antenna array with faults at same positions (i.e., 3rd and 18th) was considered. The degraded pattern due to element failure and the recovered optimized pattern with two nulls at $-42^\circ$ and $18^\circ$ are shown in Figure 9. This approach was extended for three element failure correction in antenna array (Table 4). Figure 10 shows

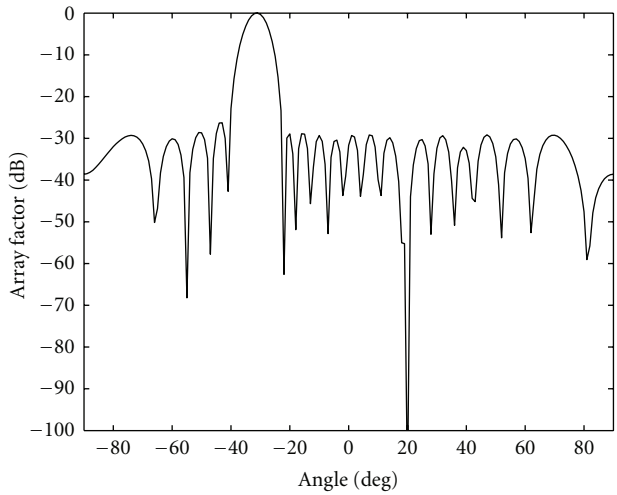


Figure 5: Radiation pattern of the 20 element linear array with null at 20°, main beam at −30° and SLL at −30 dB.

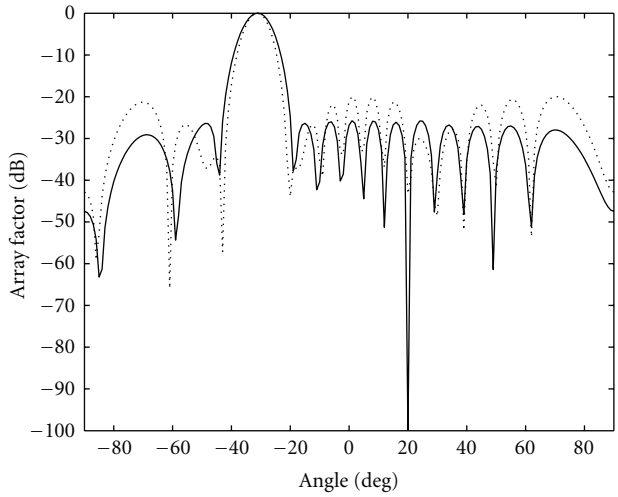


Figure 6: Radiation pattern for 3rd and 18th element failure with main beam at −30°. Dotted line curve shows the damaged array pattern and the solid line curve shows the corrected pattern.

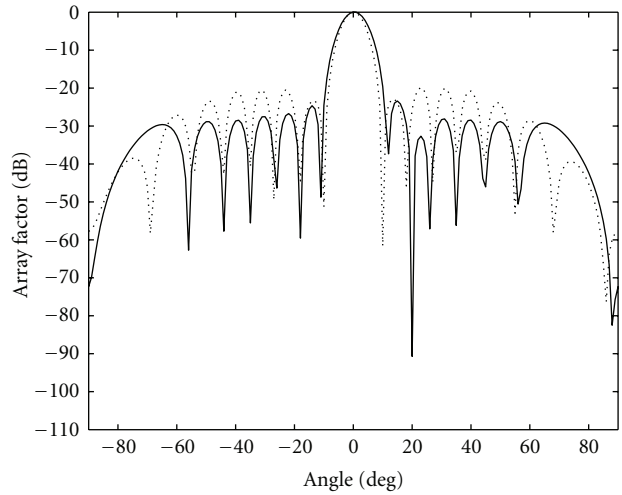


Figure 7: Radiation pattern for failures at 2nd, 3rd, 18th, and 19th element. Dotted curve shows the damaged array pattern and the solid line curve shows the corrected pattern.

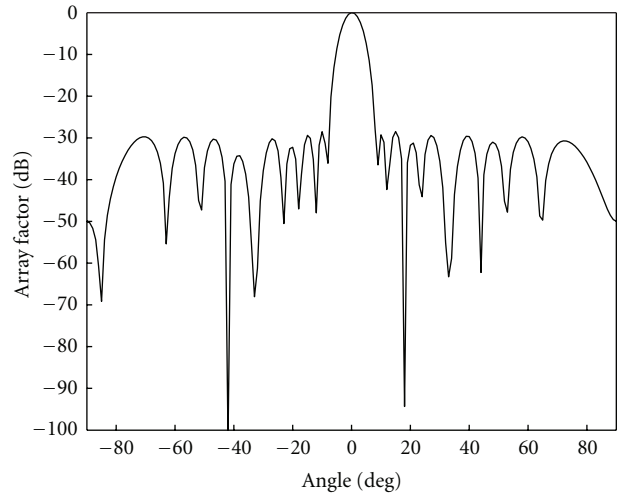


Figure 8: Radiation pattern of 20 element linear broadside array with null at −42° and 18° and SLL of −30 dB.

the results for double nulls in the presence of defective elements present at 3rd, 18th, and 19th positions of the antenna array along with the damaged pattern. Like the previous case, here also it was observed that the depth of the recovered null gets reduced with the increase in number of defective elements.

*Case 3* (recovery of triple null with element failure). The problem of single and double null recovery in a failed antenna array as discussed in Cases 1 and 2 has been extended to triple null recovery in this section. Three nulls were imposed at −20°, 33°, and 50°. The recovery behavior of these nulls in presence of fault elements at 3rd and 18th element were studied with respect to the SLL, NDL and computation time. Figures 11 and 12 show the original, defected, and the recovered pattern. The element excitations and the SLL, NDL are given in Tables 5 and 6, respectively.

*Case 4* (recovery of sectored null with element failure). Broad or sectored nulls are needed when the direction of arrival of unwanted interference signal varies slightly with time or the directions of interferers are not known exactly. The broadband interference suppression can be achieved by the application of the sector nulling methods. In the present work the pattern with broad nulls located at 30° with $\Delta\theta_i = 5°$ was obtained by perturbing the amplitude and phase of the elements of antenna array and is shown in Figure 13. It was observed that the performance of the broad null was degraded when the array elements positioned at 2, 3, and 18 became nonradiating (Table 7). Then the developed PSO-based technique was applied to reoptimize the current excitations of the remaining working elements to improve the nulling performance and to reduce the SLL (Table 8). Figure 14 shows the damaged pattern and the corrected pattern with the broad null at 30°.

Table 3: Element excitations corresponding to Case 2.

| Element positions | Double nulls at −42° and 20° without any fault | | Recovery of nulls with two faults at 3rd and 18th positions | | Recovery of nulls with three faults at 3rd, 18th and 19th positions | |
|---|---|---|---|---|---|---|
| | Amplitude | Phase (Deg) | Amplitude | Phase (Deg) | Amplitude | Phase (Deg) |
| 1 | 0.2716 | 7.1444 | 0.0154 | 0.3249 | 0.0180 | 3.0626 |
| 2 | 0.2615 | 1.9282 | 0.0691 | 1.2790 | 0.0015 | 0.6149 |
| 3 | 0.4278 | 3.9834 | **0.0000** | **0.0000** | **0.0000** | **0.0000** |
| 4 | 0.4895 | 3.8468 | 0.3100 | 7.1814 | 0.3219 | 5.6422 |
| 5 | 0.5706 | 1.8943 | 0.4580 | 0.0017 | 0.4280 | 0.0872 |
| 6 | 0.7227 | 2.8477 | 0.6239 | 1.9097 | 0.6090 | 2.8531 |
| 7 | 0.8255 | 2.3399 | 0.7192 | 3.7367 | 0.7135 | 3.1334 |
| 8 | 0.8617 | 0.9593 | 0.8410 | 0.2160 | 0.8540 | 0.4014 |
| 9 | 0.9127 | 0.8437 | 0.9825 | 1.2352 | 0.9745 | 1.0881 |
| 10 | 1.0000 | 0.9971 | 1.0000 | 1.8251 | 1.0000 | 1.2017 |
| 11 | 1.0000 | 0.9971 | 1.0000 | 1.8251 | 1.0000 | 1.2017 |
| 12 | 0.9127 | 0.8437 | 0.9825 | 1.2352 | 0.9745 | 1.0881 |
| 13 | 0.8617 | 0.9593 | 0.8410 | 0.2160 | 0.8540 | 0.4014 |
| 14 | 0.8255 | 2.3399 | 0.7192 | 3.7367 | 0.7135 | 3.1334 |
| 15 | 0.7227 | 2.8477 | 0.6239 | 1.9097 | 0.6090 | 2.8531 |
| 16 | 0.5706 | 1.8943 | 0.4580 | 0.0017 | 0.4280 | 0.0872 |
| 17 | 0.4895 | 3.8468 | 0.3100 | 7.1814 | 0.3219 | 5.6422 |
| 18 | 0.4278 | 3.9834 | **0.0000** | **0.0000** | **0.0000** | **0.0000** |
| 19 | 0.2615 | 1.9282 | 0.0691 | 1.2790 | **0.0000** | **0.0000** |
| 20 | 0.2716 | 7.1444 | 0.0154 | 0.3249 | 0.0180 | 3.0626 |

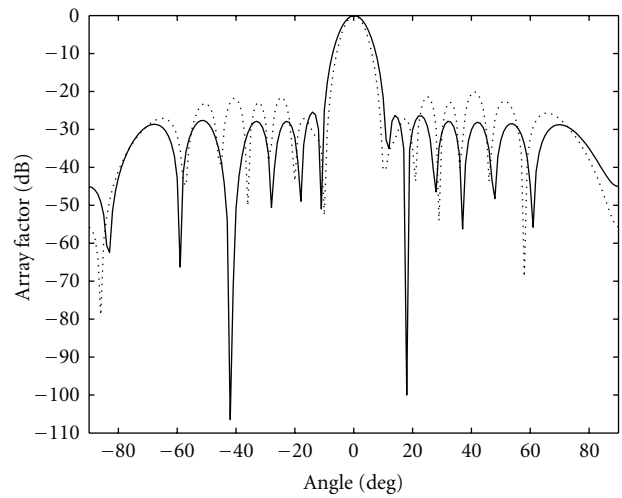


Figure 9: Radiation pattern for 3rd and 18th element failure with main beam at broadside and nulls at −42° and 18°. Dotted line curve shows the damaged array pattern and the solid line curve shows the corrected pattern.

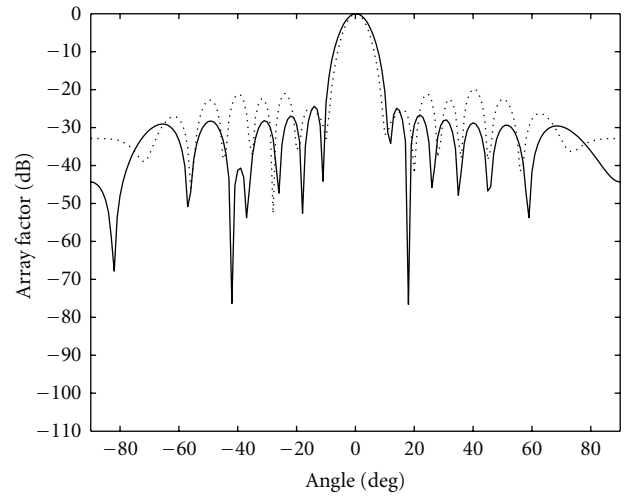


Figure 10: Radiation pattern for 3rd, 18th, and 19th element failure with main beam at broadside and nulls at −42° and 18°. Dotted line curve shows the damaged array pattern and the solid line curve shows the corrected pattern.

The four different cases of null steering described above were simulated on a 2.33 GHz workstation platform with 4 GB RAM. The computation time for these observations is given in Table 9. It was observed that the variations in computation time in all these cases are very small. The slight variation is due to the change in the position of the faulty element and the number of nulls in the array pattern.

A closer look at all these 4 cases of pattern recovery shows that, with increase in the number of nulls, the depths of the recovered null decrease and at the same time average SLL gradually increases more from the fixed value of SLL for the Chebyshev array. A common observation from the available literature [11, 12, 14] for null steering without any faulty element, was that the SLL increases from specified level to

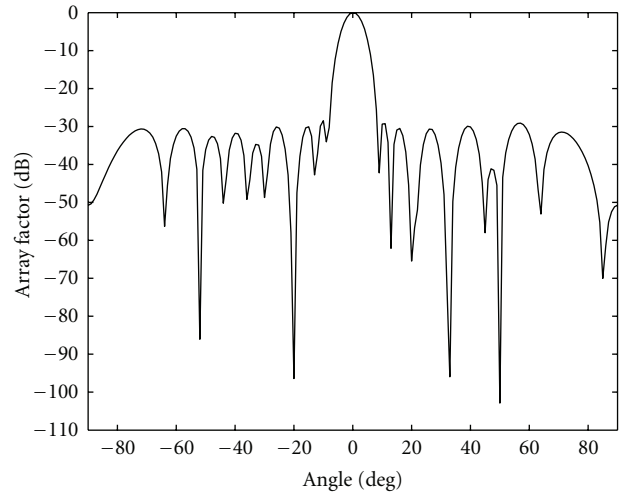


Figure 11: Radiation pattern of the same linear array with imposed nulls at −20°, 33°, and 50°.

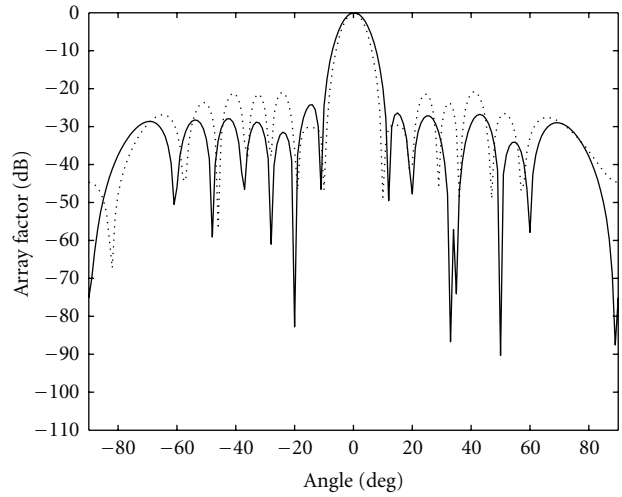


Figure 12: Radiation pattern for 3rd, and 18th element failure with main beam at broadside and nulls at −20°, 33° and 50°. Dotted line curve shows the damaged array pattern and the solid line curve shows the corrected pattern.

Table 4: Comparison of NDL and SLL for the configurations discussed in Case 2.

| | Without any fault | | With failure of two elements | | With failure of three elements | |
|---|---|---|---|---|---|---|
| | −42° | 18° | −42° | 18° | −42° | 18° |
| NDL (dB) | −102.2 | −93.12 | −106 | −100 | −76.35 | −76.61 |
| SLL (dB) | −28.51 | | −25.45 | | −24.95 | |

accommodate the nulls in the pattern. In the present work also, we observed the similar variations in the pattern for the array without any fault while imposing nulls. As we extended our work for failed array, the recovered SLL was slightly at higher level. So the user has to compromise with the number of actual null required for the application.

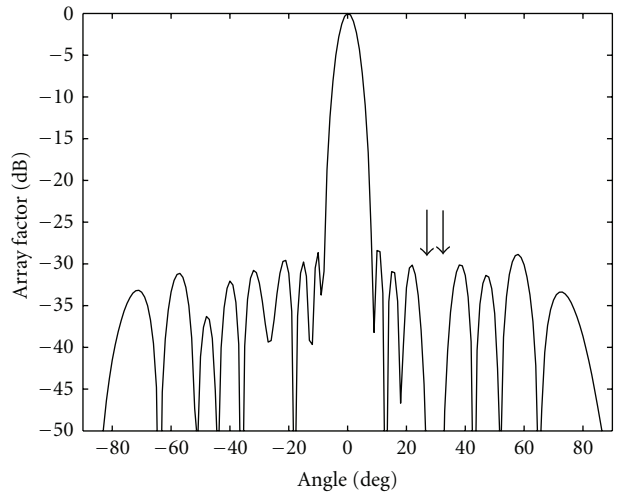


Figure 13: Radiation pattern of 20-element linear broadside array with a broad null at 30°.

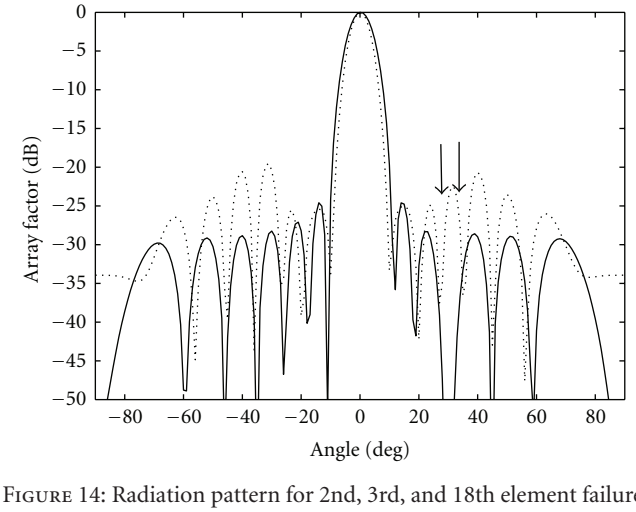


Figure 14: Radiation pattern for 2nd, 3rd, and 18th element failure with main beam at broadside and broad null at 30°. Dotted line curve shows the damaged array pattern and the solid line curve shows the corrected pattern.

## 5. Conclusion

The problem of maintaining null positions and SLL suppression in failed antenna array was approached as an optimization problem and solved successfully using PSO. The role of PSO was to find the optimized set of the amplitude and phase excitations of the working elements in the array to recover the desired pattern. In this process of compensation the SLL was reduced and null was restored at its original position. The developed technique gives the performance of pattern restoration in faulty arrays which is at par with the performance obtained by antennas without any fault

Table 5: Element excitations corresponding to Case 3.

| Element positions | Triple nulls at −20°, 33°, and 50° without any fault | | Recovery of nulls with two faults at 3rd and 18th positions | |
|---|---|---|---|---|
| | Amplitude | Phase (Deg) | Amplitude | Phase (Deg) |
| 1 | 0.2310 | 0.9933 | 0.0087 | 0.2746 |
| 2 | 0.2177 | 7.3854 | 0.0942 | 9.2318 |
| 3 | 0.3708 | 2.4157 | **0.0000** | **0.0000** |
| 4 | 0.4754 | 1.9392 | 0.2553 | 0.6650 |
| 5 | 0.6012 | 2.4845 | 0.4233 | 5.7740 |
| 6 | 0.6985 | 2.3370 | 0.5877 | 3.7755 |
| 7 | 0.7743 | 2.0885 | 0.7472 | 2.5436 |
| 8 | 0.8421 | 0.0284 | 0.8541 | 1.0084 |
| 9 | 0.8801 | 0.5122 | 0.9004 | 2.8874 |
| 10 | 1.0000 | 1.5159 | 1.0000 | 2.7783 |
| 11 | 1.0000 | 1.5159 | 1.0000 | 2.7783 |
| 12 | 0.8801 | 0.5122 | 0.9004 | 2.8874 |
| 13 | 0.8421 | 0.0284 | 0.8541 | 1.0084 |
| 14 | 0.7743 | 2.0885 | 0.7472 | 2.5436 |
| 15 | 0.6985 | 2.3370 | 0.5877 | 3.7755 |
| 16 | 0.6012 | 2.4845 | 0.4233 | 5.7740 |
| 17 | 0.4754 | 1.9392 | 0.2553 | 0.6650 |
| 18 | 0.3708 | 2.4157 | **0.0000** | **0.0000** |
| 19 | 0.2177 | 7.3854 | 0.0942 | 9.2318 |
| 20 | 0.2310 | 0.9933 | 0.0087 | 0.2746 |

Table 6: Comparison of NDL and SLL for the configurations discussed in Case 3.

| | Without failure | | | With failure of two elements | | |
|---|---|---|---|---|---|---|
| | −20° | 33° | 50° | −20° | 33° | 50° |
| NDL (dB) | −96.43 | −95.96 | −102.9 | −82.78 | −86.76 | −90.28 |
| SLL (dB) | | −28.48 | | | −24.37 | |

Table 7: Element excitations corresponding to Case 4.

| Element positions | Broad Null centered at 30° without fault | | Broad Null centered at 30° with three element failure | |
|---|---|---|---|---|
| | Amplitude | Phase (Deg) | Amplitude | Phase (Deg) |
| 1 | 0.2344 | 1.9155 | 0.0004 | 7.6577 |
| 2 | 0.2397 | 5.5728 | **0.0000** | **0.0000** |
| 3 | 0.4296 | 5.3054 | **0.0000** | **0.0000** |
| 4 | 0.5450 | 0.3482 | 0.3103 | 0.0590 |
| 5 | 0.5963 | 3.2661 | 0.3985 | 6.4968 |
| 6 | 0.7083 | 3.7560 | 0.5793 | 5.6558 |
| 7 | 0.8404 | 0.1983 | 0.7340 | 1.4852 |
| 8 | 0.9752 | 0.0291 | 0.8283 | 0.7896 |
| 9 | 0.9782 | 1.3469 | 0.9221 | 1.8630 |
| 10 | 1.0000 | 1.2506 | 1.0000 | 1.2461 |
| 11 | 1.0000 | 1.2506 | 1.0000 | 1.2461 |
| 12 | 0.9782 | 1.3469 | 0.9221 | 1.8630 |
| 13 | 0.9752 | 0.0291 | 0.8283 | 0.7896 |
| 14 | 0.8404 | 0.1983 | 0.7340 | 1.4852 |
| 15 | 0.7083 | 3.7560 | 0.5793 | 5.6558 |
| 16 | 0.5963 | 3.2661 | 0.3985 | 6.4968 |
| 17 | 0.5450 | 0.3482 | 0.3103 | 0.0590 |
| 18 | 0.4296 | 5.3054 | **0.0000** | **0.0000** |
| 19 | 0.2397 | 5.5728 | 0.0168 | 0.8837 |
| 20 | 0.2344 | 1.9155 | 0.0004 | 7.6577 |

Table 8: Comparison of NDL and SLL for the configurations discussed in Case 4.

| | Without failure | With failure of three elements |
|---|---|---|
| NDL (dB) | −71.03 | −63.1 |
| SLL (dB) | −28.65 | −24.77 |

Table 9: Computational time for the configurations discussed in Cases 1–4.

| Cases | Faulty element positions | Computational time (Sec) |
|---|---|---|
| Case 1 (single null) | Two element failure (3rd and 18th) | 28.96 |
| | Four element failure (2nd, 3rd, 18th, and 19th) | 29.04 |
| Case 2 (double null) | Two element failure (3rd and 18th) | 29.08 |
| | Three element failure (3rd, 18th, and 19th) | 30.34 |
| Case 2 (triple null) | Two element failure (3rd and 18th) | 29.16 |
| Case 2 (broad null) | Three element failure (2nd, 3rd, and 18th) | 31.12 |

elements. It was observed that the computation time of this method depends on number of failed elements and the position of the failed elements. The proposed technique is simple and easy to implement and can be extended for arrays with complex geometry by modifying the associated evaluation function. The developed methodology can be helpful in increasing the life span of the arrays, particularly for the arrays without direct human access. At the same time it can save the hardware replacement cost also.

## Acknowledgments

This work is done as a part of a technology development project from the Naval Research Board, DRDO, and Govternment of India through Grant no. NRB-176/SSB/08-09. The authors appreciates the constructive comments of the reviewer, which helped improving the quality of the paper.

## References


[1] C. A. Balanis, *Antenna Theory Analysis and Design*, John Wiley & Sons, New York, NY, USA, 2005.

[2] H. Steyskal, R. A. Shore, and R. L. Haupt, "Methods for null control and their effects on the radiation pattern," *IEEE Transactions on Antennas and Propagation*, vol. 34, no. 3, pp. 404–409, 1986.

[3] H. M. Ibrahim, "Null steering by real-weight control—a method of decoupling the weights," *IEEE Transactions on Antennas and Propagation*, vol. 39, no. 11, pp. 1648–1650, 1991.

[4] H. Steyskal, "Simple method for pattern nulling by phase perturbations," *IEEE Transactions on Antennas and Propagation*, vol. 31, no. 1, pp. 163–166, 1983.

[5] R. A. Shore, "Nulling at symmetric pattern location with phase-only weight control," *IEEE Transactions on Antennas and Propagation*, vol. 32, no. 5, pp. 530–533, 1984.

[6] T. H. Ismail and M. M. Dawoud, "Null steering in phased arrays by controlling the element positions," *IEEE Transactions on Antennas and Propagation*, vol. 39, no. 11, pp. 1561–1566, 1991.

[7] R. L. Haupt, "Phase-only adaptive nulling with a genetic algorithm," *IEEE Transactions on Antennas and Propagation*, vol. 45, no. 6, pp. 1009–1015, 1997.

[8] W. P. Liao and F. L. Chu, "Array pattern nulling by phase and position perturbations with the use of the genetic algorithm," *Microwave and Optical Technology Letters*, vol. 15, no. 4, pp. 251–256, 1997.

[9] A. Tennant, M. M. Dawoud, and A. P. Anderson, "Array pattern nulling by element position perturbation using genetic algorithm," *Microwave and Optical Technology Letters*, vol. 15, no. 4, pp. 251–256, 1997.

[10] B. Babayigit, A. Akdagli, and K. Guney, "A clonal selection algorithm for null synthesizing of linear antenna arrays by amplitude control," *Journal of Electromagnetic Waves and Applications*, vol. 20, no. 8, pp. 1007–1020, 2006.

[11] K. Guney and S. Basbug, "Interference suppression of linear antenna arrays by amplitude-only control using a bacterial foraging algorithm," *Progress in Electromagnetics Research*, vol. 79, pp. 475–497, 2008.

[12] K. Guney and M. Onay, "Amplitude-only pattern nulling of linear antenna arrays with the use of bees algorithm," *Progress in Electromagnetics Research*, vol. 70, pp. 21–36, 2007.

[13] M. M. Khodier and C. G. Christodoulou, "Linear array geometry synthesis with minimum sidelobe level and null control using particle swarm optimization," *IEEE Transactions on Antennas and Propagation*, vol. 53, no. 8, pp. 2674–2679, 2005.

[14] D. Karaboga, K. Guney, and A. Akdagli, "Antenna array pattern nulling by controlling both amplitude and phase using modified touring ant colony optimization algorithm," *International Journal of Electronics*, vol. 91, no. 4, pp. 241–251, 2004.

[15] K. Guney, B. Babayigit, and A. Akdagli, "Interference suppression of linear antenna arrays by phase-only control using a clonal selection algorithm," *Journal of the Franklin Institute*, vol. 345, no. 3, pp. 254–266, 2008.

[16] R. J. Mailloux, *Phased Array Antennas Handbook*, Artech House, Norwood, Mass, USA, 1994.

[17] R. J. Mailloux, "Array failure correction with a digitally beamformed array," *IEEE Transactions on Antennas and Propagation*, vol. 44, no. 12, pp. 1542–1550, 1996.

[18] H. Steyskal and R. J. Mailloux, "Generalization of an array failure correction method," *IEE Proceedings Microwaves, Antennas & Propagation*, vol. 145, no. 4, pp. 332–336, 1998.

[19] T. J. Peters, "A conjugate gradient-based algorithm to minimize the sidelobe level of planar arrays with element failures," *IEEE Transactions on Antennas and Propagation*, vol. 39, no. 10, pp. 1497–1504, 1991.

[20] S. H. Zainud-Deen, M. S. Ibrahem, H. A. Sharshar, and S. M. M. Ibrahem, "Array failure correction with orthogonal method," in *Proceedings of the Twenty First National Radio Science Conference, (NRSC '04)*, pp. 1–9, Cairo, Egypt, March 2004.

[21] M. Levitas, D. A. Horton, and T. C. Cheston, "Practical failure compensation in active phased arrays," *IEEE Transactions on Antennas and Propagation*, vol. 47, no. 3, pp. 524–535, 1999.

[22] B. K. Yeo and Y. Lu, "Array failure correction with a genetic algorithm," *IEEE Transactions on Antennas and Propagation*, vol. 47, no. 5, pp. 823–828, 1999.

[23] J. A. Rodriguez, F. Ares, E. Moreno, and G. Franceschetti, "Genetic algorithm procedure for linear array failure correction," *Electronics Letters*, vol. 36, no. 3, pp. 196–198, 2000.

[24] J. A. Rodriguez and F. Ares, "Optimization of the performance of arrays with failed elements using the simulated annealing technique," *Journal of Electromagnetic Waves and Applications*, vol. 12, no. 12, pp. 1625–1638, 1998.

[25] B. K. Yeo and Y. Lu, "Adaptive array digital beamforming using complex-coded particle swarm optimization-genetic algorithm," in *Proceedings of the Asia-Pacific Microwave Conference, (APMC '05)*, pp. 4–7, Suzhou, China, December 2005.

[26] L. L. Wang and D. G. Fang, "Combination of genetic algorithm and fast fourier transform for array failure correction," in *Proceedings of the 6th International Symposium on Antennas, Propagation and EM Theory*, Beijing, China, November 2003.

[27] J. Kennedy and R. C. Eberhart, "Particle swarm optimization," in *Proceedings of the IEEE International Conference on Neural Networks IV, (ICNN '95)*, Piscataway, NJ, USA, December 1995.

[28] R. C. Eberhart and Y. Shi, "Particle swarm optimization: developments, applications and resources," in *Proceedings of the Congress on Evolutionary Computation*, vol. 1, Seoul, Korea, May 2001.

[29] R. C. Eberhart and Y. Shi, "Comparing inertia weights and constriction factors in particle swarm optimization," in *Proceedings of the Congress on Evolutionary Computation*, pp. 84–88, San Diego, Calif, USA, July 2000.

[30] J. Robinson and Y. Rahmat-Samii, "Particle swarm optimization in electromagnetics," *IEEE Transactions on Antennas and Propagation*, vol. 52, no. 2, pp. 397–407, 2004.

[31] J. Kennedy and W. M. Spears, "Matching algorithms to problems: an experimental test of the particle swarm and some genetic algorithms on the multimodal problem generator," in *Proceedings of the IEEE International Conference on Evolutionary Computation, (ICEC'98)*, Anchorage, Alaska, USA, May 1998.